Detailed experimental results and proofs

EC.1. Missing proofs

EC.1.1. Proof of Theorem 1

Following the notation introduced in the paper, we denote $\{y \in \mathcal{Y} \,|\, (d^\theta)^\top y \leq C - b^\top \theta\}$ as $\mathcal{Y}_\theta$. Let us first prove $\mathcal{Y} \subseteq \bigcup_{\theta \in \Theta} \mathcal{Y}_\theta$. Hence, let $y \in \mathcal{Y}$, $\xi^* \in \arg\max_{\xi \in \Xi} \left\{ \sum_{i=1}^{n} \hat{d}_i \xi_i y_i \right\}$, and (θ^*, z^*) be an optimal solution of the dual of the latter maximization problem such that $\theta^* \in \Theta$. Such an optimal solution exists because the dual of the previous maximization problem is equivalent to the left-hand side of (4), the latter problem minimizing a convex piecewise linear function whose breakpoints belong to Θ. By the strong duality of linear programming, we have that

$$b^\top \theta^* + (d^{\theta^*})^\top y = \bar{d}^\top y + b^\top \theta^* + \sum_{i=1}^{n} z^* = \bar{d}^\top y + \sum_{i=1}^{n} \hat{d}_i \xi_i^* y_i \leq C,$$

where the last inequality holds because $y \in \mathcal{Y}$. Thus, $y \in \mathcal{Y}_{\theta^*}$.

To prove the reverse inclusion, let $y \in \mathcal{Y}_{\theta'}$ for some $\theta' \in \Theta$. We have that

$$\begin{aligned} \bar{d}^\top y + \max_{\xi \in \Xi} \left\{ \sum_{i=1}^{n} \hat{d}_i \xi_i y_i \right\} = \\ \bar{d}^\top y + \min_{\theta \in \mathbb{R}^s_+} \left\{ b^\top \theta + \sum_{i=1}^{n} \max\{0, \hat{d}_i - w_i \theta_{k(i)}\} y_i \right\} \leq \\ \bar{d}^\top y + b^\top \theta' + \sum_{i=1}^{n} \max\{0, \hat{d}_i - w_i \theta'_{k(i)}\} y_i = \\ b^\top \theta' + (d^{\theta'})^\top y \leq C. \end{aligned}$$

As a result, $y \in \mathcal{Y}$, finishing the proof. □

EC.1.2. Proof of Theorem 3

Recall the notation $\mathcal{Y}_\theta \equiv \{y \in \mathcal{Y} \,|\, (d^\theta)^\top y \leq C - b^\top \theta\}$. Analyzing the proof of Theorem 1, we see that not all $\theta \in \Theta$ are needed in the decomposition formulated in the theorem, but only those which belong to the set

$$\Theta' \equiv \bigcup_{y \in Y} \arg\min_{\theta \in \Theta} b^\top \theta + (d^\theta)^\top y.$$

Hence, the proof of Theorem 1 leads immediately to the following result.

COROLLARY EC.1. $\mathcal{Y} = \bigcup_{\theta \in \Theta'} \mathcal{Y}_\theta$

Next, we prove that $\tilde{\mathcal{Y}}_\theta = \mathcal{Y}_\theta$ for each $\theta \in \Theta'$.

PROPOSITION EC.1. *Let $\theta \in \Theta'$. It holds that $\tilde{\mathcal{Y}}_\theta = \mathcal{Y}_\theta$.*

Proof. Recall that

$$\tilde{\mathcal{Y}}_\theta \equiv \left\{ y \in \mathcal{Y}_\theta \,\middle|\, b_k \leq \sum_{i \in V_k : \hat{d}_i \geq \theta_k} w_i y_i, \forall k \in \{\ell \in \{1,\dots,s\} \,|\, \theta_\ell > 0\} \right\}.$$

By definition, $\tilde{\mathcal{Y}}_\theta \subseteq \mathcal{Y}_\theta$ for any $\theta \in \Theta$. To prove the reverse inclusion, let ξ^* be an optimal solution to the adversarial problem

$$\max_{\xi \in [0,1]^n} \left\{ \sum_{i=1}^n \xi_i \hat{d}_i y_i \text{ s.t. } \sum_{i \in V_k} w_i \xi_i \leq b_k,\ k = 1,\dots,s \right\} \tag{EC.1}$$

and (θ^*, z^*) be an optimal solution to the dual problem

$$\min_{\theta, z \geq 0} \left\{ b^\top \theta + \sum_{i=1}^n z_i \text{ s.t. } z_i + w_i \theta_{k(i)} \geq \hat{d}_i y_i, \quad i = 1,\dots,n \right\}. \tag{EC.2}$$

The complementary slackness conditions imply that

$$\theta^*_k > 0 \implies \sum_{i \in V_k} w_i \xi^*_i = b_k \tag{EC.3}$$

for $k = 1,\dots,s$, and

$$\xi^*_i > 0 \implies z^*_i + w_i \theta^*_{k(i)} = \hat{d}_i y_i, \tag{EC.4}$$

for $i = 1,\dots,n$. Consider any vector $y \in \mathcal{Y}_\theta$. We can assume w.l.o.g. that the optimal solution ξ^* is such that $y_i = 0 \implies \xi^*_i = 0$, which is equivalent to

$$\xi^*_i > 0 \implies y_i = 1. \tag{EC.5}$$

Consider $k \in \{1,\dots,s\}$ such that $\theta^*_k > 0$. Applying subsequently (EC.3), $\xi^* \leq 1$, and (EC.5), we obtain that y satisfies the following constraint

$$b_k = \sum_{i \in V_k} w_i \xi^*_i \leq \sum_{i \in V_k : \xi^*_i > 0} w_i = \sum_{i \in V_k : \xi^*_i > 0} w_i y_i. \tag{EC.6}$$

Using (EC.5) and $z^* \geq 0$, (EC.4) can be reformulated as $\xi_i^* > 0 \implies w_i\theta^*_{k(i)} \leq \hat{d}_i$, so that

$$\{i \in V_k : \xi_i^* > 0\} \subseteq \{i \in V_k : \hat{d}_i \geq w_i\theta_k^*\}. \tag{EC.7}$$

Combining (EC.7) with (EC.6) leads immediately to

$$b_k \leq \sum_{i \in V_k : \hat{d}_i \geq w_i\theta_k^*} w_i y_i.$$

□

Proof of Theorem 3. From Corollary EC.1, we have that $\mathcal{Y} = \bigcup_{\theta \in \Theta' : \mathcal{Y}_\theta \neq \emptyset} \mathcal{Y}_\theta$. Using Proposition EC.1, we rewrite the latter as $\mathcal{Y} = \bigcup_{\theta \in \Theta' : \tilde{\mathcal{Y}}_\theta \neq \emptyset} \mathcal{Y}_\theta$, and the result follows from $\Theta' \subseteq \Theta$. □

Out of completeness we provide a stronger variant of Proposition EC.1 below, showing that for $\theta \in \Theta'$, any $y \in \mathcal{Y}$ satisfies additional constraints.

Proposition EC.2. *Let $\theta \in \Theta'$. It holds that*

$$\mathcal{Y}_\theta = \left\{ y \in \tilde{\mathcal{Y}}_\theta \;\middle|\; \sum_{i \in V_k} w_i y_i \leq b_k, \forall k \in \{\ell \in \{1,\dots,s\} \,|\, \theta_\ell = 0\}, \sum_{\substack{i \in V_k \\ \hat{d}_i > w_i\theta_k}} w_i y_i \leq b_k, \forall k \in \{\ell \in \{1,\dots,s\} \,|\, \theta_\ell > 0\} \right\}.$$

Proof. Let ξ^*, z^*, θ^* and y be as in the proof of Proposition EC.1 and consider $k \in \{1,\dots,s\}$ such that $\theta_k^* > 0$. Applying subsequently (EC.3) and (EC.5), we obtain that y satisfies the following constraint

$$b_k = \sum_{i \in V_k} w_i \xi_i^* \geq \sum_{i \in V_k : \xi_i^* = 1} w_i = \sum_{i \in V_k : \xi_i^* = 1} w_i y_i. \tag{EC.8}$$

Let us introduce the additional complementary slackness condition

$$z_i^* > 0 \implies \xi_i^* = 1. \tag{EC.9}$$

If $y_i = 1$ and $\hat{d}_i > w_i\theta_k^*$, then $z_i > 0$, so that (EC.9) yields $\xi_i^* = 1$. Therefore,

$$\{i \in V_k : \xi_i^* = 1\} \supseteq \{i \in V_k : \hat{d}_i > w_i\theta_k^*,\, y_i = 1\}. \tag{EC.10}$$

Combining (EC.10) with (EC.8) leads immediately to

$$b_k \geq \sum_{i \in V_k : \hat{d}_i > w_i\theta_k^*,\, y_i = 1} w_i y_i = \sum_{i \in V_k : \hat{d}_i > w_i\theta_k^*} w_i y_i.$$

Consider next $k \in \{1,\dots,s\}$ such that $\theta_k^* = 0$. We prove first that for each $i \in V_k$

$$y_i = 1 \implies \xi_i^* = 1. \tag{EC.11}$$

Linear programs (EC.1) and (EC.2) are decomposable by $k \in \{1,\dots,s\}$ and the strong duality holds for each $k \in \{1,\dots,s\}$ so that

$$\sum_{i \in V_k} \xi_i^* \hat{d}_i y_i = b_k \theta_k^* + \sum_{i \in V_k} z_i^*.$$

From $\theta_k^* = 0$, we have that $z_i^* = \hat{d}_i y_i$ for each $i \in V_k$, so the above equation becomes

$$\sum_{i \in V_k} \xi_i^* \hat{d}_i y_i = \sum_{i \in V_k} \hat{d}_i y_i,$$

which is true only if (EC.11) holds. From (EC.11), we obtain

$$b_k \geq \sum_{i \in V_k} w_i \xi_i^* \geq \sum_{i \in V_k} w_i y_i.$$

□

Notice that the above proposition has not been used in our numerical experiments since they rely on testing the feasibility of the larger set $\hat{\mathcal{Y}}_\theta$.

EC.1.3. Proof of Lemma 1

Testing the feasibility of $\hat{\mathcal{Y}}_\theta$ can be done by solving

$$z^* = \min_{y \in \{0,1\}^n} \left\{ (d^\theta)^\top y \;\middle|\; \sum_{i \in \hat{V}_k(\theta)} w_i y_i \geq b_k, \forall k \in K(\theta) \right\} = \sum_{k \in K(\theta)} \min_{y \in \{0,1\}^{|V_k|}} \left\{ \sum_{i \in V_k} d_i^\theta y_i \;\middle|\; \sum_{i \in \hat{V}_k(\theta)} w_i y_i \geq b_k \right\} \tag{EC.12}$$

$$= \sum_{k \in K(\theta)} \min_{y \in \{0,1\}^{|\hat{V}_k(\theta)|}} \left\{ \sum_{i \in \hat{V}_k(\theta)} d_i^\theta y_i \;\middle|\; \sum_{i \in \hat{V}_k(\theta)} w_i y_i \geq b_k \right\}, \tag{EC.13}$$

where the second equality holds because $d_i^\theta \geq 0$, so we can put to 0 all components of y not appearing in the constraint. Let z_k^* be the optimal solution cost of the k-th knapsack problem considered in (EC.13). The value z^* can be computed in pseudo-polynomial time by solving a knapsack problem for each $k \in K(\theta)$. If one of these knapsack problems is infeasible, then we set $z_k^* = \infty$. Then, having $z^* > C - b^\top \theta$ implies that $\hat{\mathcal{Y}}_\theta$ is empty.

EC.1.4. Proof of Lemma 2

Clearly, Θ^{card} satisfies the hypothesis of Theorem 3 whenever $s=1$, $b_1=\Gamma$, and $w_1=\cdots=w_n=1$. Therefore, one can conclude that $\hat{\mathcal{Y}}_\theta$ is empty (for $\theta>0$) whenever

$$\min_{y\in\{0,1\}^n}\left\{\sum_{i\in\{1,\ldots,n\}:\hat{d}_i\geq\theta} d_i^\theta y_i \;\middle|\; \sum_{i\in\{1,\ldots,n\}:\hat{d}_i\geq\theta} y_i=\Gamma\right\} > C-\Gamma\theta.$$

Note that the minimum is attained at the left-hand side of the previous inequality when $y_i=1$ for the indices i that correspond to the Γ smallest values of $\hat{d}_i$ that are not smaller than θ. □

EC.1.5. Proof of Lemma 3

In the case of $\mathcal{D}^{part}$, we see that $\theta^i_{k(i)}=1$ for each $i\in V_k$ and $k\in K(\theta)$, so that $\hat{V}_k(\theta)=V_k$ and $d^\theta=\bar{d}$. Now, we further assume that $\hat{d}=\kappa\bar{d}$ for some scalar $\kappa>0$ (which is true for all current literature instances), and consider the linear relaxation of the of $\hat{\mathcal{Y}}_\theta$ written for for $\mathcal{D}^{part}$

$$\hat{\mathcal{Y}}^{LP}_\theta \equiv \left\{ y\in[0,1]^n \,|\, b^\top\theta + \bar{d}^\top y \leq C, \sum_{i\in V_k}\kappa\bar{d}_i y_i \geq b_k, \forall k\in K(\theta)\right\}.$$

Clearly, $\hat{\mathcal{Y}}_\theta\subseteq\hat{\mathcal{Y}}^{LP}_\theta$. What is more

$$z^*_k = \min_{y\in[0,1]^{|V_k|}}\left\{\sum_{i\in V_k}\bar{d}_i y_i \;\middle|\; \sum_{i\in V_k}\kappa\bar{d}_i y_i\geq b_k\right\} = b_k/\kappa$$

for each $k\in K(\theta)$, so that the counterpart of z^* for $\mathcal{D}^{part}$ is $\sum_{k\in K(\theta)} b_k/\kappa = (b^\top\theta)/\kappa$. Hence, $\hat{\mathcal{Y}}^{LP}_\theta$ is necessarily empty when $(b^\top\theta)/\kappa > C-b^\top\theta$. □

EC.1.6. Proof of Theorem 4

We provide next a lower bound on the number of vehicles required to cover the customers of S. Having the heterogeneous formulation (14)–(17) in mind, our bound is based on an integer program specifying how many vehicles of each type one needs to cover all customers. Specifically, for each vehicle type $\theta\in\tilde{\Theta}$ we introduce the integer variable w_θ which represents how many vehicles of type θ are used, each of which having a capacity $C-b^\top\theta$, and the binary variable $v_{i\theta}$ which is equal to 1 iff customer i is assigned to a vehicle of type θ. In particular, the formulation does not assign customers to specific vehicles, only to types. We obtain

$$\check{r}(S) = \min \quad \sum_{\theta\in\tilde{\Theta}} w_\theta, \tag{EC.14}$$

$$\text{s.t.} \quad \sum_{\theta\in\tilde{\Theta}} v_{i\theta} \geq 1, \quad i \in S, \qquad (\mu_i) \tag{EC.15}$$

$$\sum_{i\in S} d_i^\theta v_{i\theta} \leq (C - b^\top\theta) w_\theta, \quad \theta \in \tilde{\Theta}, \qquad (\nu_\theta) \tag{EC.16}$$

$$w_\theta \in \mathbb{Z},\ \theta \in \tilde{\Theta},\ v_{i\theta} \in \mathbb{Z},\ i \in V, \theta \in \tilde{\Theta}. \tag{EC.17}$$

where the corresponding dual variables of the continuous relaxation are denoted between parenthesis. In this formulation, (EC.14) represents the minimum number of routes required to serve S, (EC.15) ensures that every customer in S is served, and (EC.16) avoids using more than the available capacity for each $\theta \in \tilde{\Theta}$. The value $\check{r}(S)$ is the ideal value one would like to put in the right-hand-side of (18) since it states how many vehicles are needed to serve all customers of S, taking only into account the type of vehicle each customer is assigned to. Unfortuntaly, computing $\check{r}(S)$ requires solving the integer program (EC.14)–(EC.17), which is impractical. Therefore, we consider instead the continuous relaxation of (EC.14)–(EC.17), the optimal solution of which we denote $\dot{r}(S)$. Taking the dual of the continuous relaxation of (EC.14)–(EC.17), we obtain

$$\begin{aligned}
\dot{r}(S) = \max \quad & \sum_{i\in S} \mu_i, \\
\text{s.t.} \quad & \mu_i \leq d_i^\theta \, \nu_\theta, \quad i \in S, \theta \in \tilde{\Theta}, \\
& (C - b^\top\theta) \, \nu_\theta \leq 1, \quad \theta \in \tilde{\Theta}, \\
& \mu, \nu \geq 0.
\end{aligned}$$

Clearly, $\dot{r}(S) \leq \check{r}(S)$, so $\dot{r}(S)$ is a valid value for the right-hand-side of (18). What is more, in any optimal solution of the dual, we have $\nu_\theta = \frac{1}{C - b^\top\theta}$ and $\mu_i = \min_{\theta\in\tilde{\Theta}} d_i^\theta \, \nu_\theta$ yielding

$$\dot{r}(S) = \sum_{i\in S} \min_{\theta\in\tilde{\Theta}} \frac{d_i^\theta}{C - b^\top\theta}. \tag{EC.18}$$

□

EC.1.7. Proof of Theorem 5

In order to be able to prove the theorem, we define a new optimization problem that turns out to be a relaxation of the problem of assigning the vertices of S to the minimum number of routes,

respecting the vehicle capacities for demands in $\mathcal{D}^{part} = \{d = \bar{d} + \xi \mid \sum_{i \in V_k} \xi_i \leq b_k, k = 1, \ldots, s, \xi \leq \kappa \bar{d}\}$. We call it the *Stripe Crossing Problem* (SCP).

In SCP, we are given s striped boards, where board k has height $q_k(S)$, for $k = 1, \ldots, s$. Each board k has alternated gray and white horizontal stripes, the lowest one being gray. All gray stripes in board k have height $\frac{b_k}{\kappa}$, and all its white stripes have height $\max\{0, C - \frac{1+\kappa}{\kappa} b_k\}$, for $k = 1, \ldots, s$. Only the highest stripe may have a truncated height if it does not fit into the remaining board space. Note that board k is completely gray if $C \leq \frac{1+\kappa}{\kappa} b_k$. SCP asks for a way to draw vertical lines crossing all stripes of all boards, from bottom to top, minimizing the number of used pens. It is assumed that each pen has a limited amount C of ink, and spends 1 and $1 + \kappa$ units of ink per line length unit in white and gray stripes, respectively. Moreover, each pen is allowed to draw at most one contiguous line segment in each board. Figure EC.1 illustrates SCP by depicting an instance with 3 boards and a solution using 6 pens. The stripe heights of board 1 and the height of board 3 are indicated in the figure. Drawn lines are represented as wide dark-gray vertical lines with the corresponding pen indicated on the right.

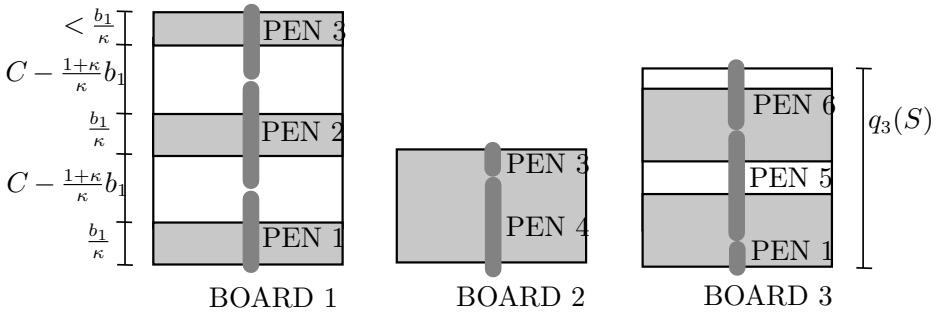

Figure EC.1 A Stripe Crossing Problem instance.

Next, we present two propositions that demonstrate the link between SCP and the minimum number of vehicles required to serve all customers in a given set S. In this link, boards represent partitions, pens represent vehicles, gray stripes represent demands that deviate in a gives scenario, and white stripes represent demands that do not deviate from their mean values. We also give an additional proposition proving that the newly proposed inequality strictly dominates (20).

PROPOSITION EC.3. *The total line length drawn with a given pen over the gray stripes of a given board is at most* $\frac{b_k}{\kappa}$.

Proof. If $C \leq \frac{1+\kappa}{\kappa} b_k$, the proposition holds because the pen spends $1+\kappa$ ink per length unit, being limited to a total length of $\frac{C}{1+\kappa} \leq \frac{b_k}{\kappa}$. Otherwise, suppose that a given pen draws a line length $\ell > \frac{b_k}{\kappa}$ over the gray stripes of a board k. Since the height of any gray stripe in this board is not greater than $\frac{b_k}{\kappa}$, the pen has to cross one of its white stripes completely. For that, it must spend at least $C - \frac{1+\kappa}{\kappa} b_k + (1+\kappa)\ell > C$, which contradicts the limit on the amount of available ink for this pen, finishing the proof. □

PROPOSITION EC.4. *The optimal solution* $r^*(S)$ *of SCP is a lower bound on the number of routes required to serve all customers in* S *in the robust CVRP with the uncertainty set* $\mathcal{D}^{part}$.

Proof. Let y be a variable matrix representing a feasible solution for the robust CVRP with $\mathcal{D}^{part}$, where $y_{\ell i} = 1$ if vertex $i \in V^0$ is served by route $\ell \in \{1, \ldots, m\}$, and 0 otherwise. We assume w.l.o.g. that routes $\ell = 1, \ldots, r$, and only them, visit S. Then, it is enough to prove that there is a feasible solution to the corresponding SCP instance using r pens.

Associate each pen with a route ℓ, for $\ell = 1, \ldots, r$. Then, for each board k, build a crossing vertical line by concatenating line segments drawn by all pens, such that the length of the line segment drawn by pen ℓ is given by $\sum_{i \in S \cap V_k} \bar{d}_i y_{\ell i}$. Note that the total line length drawn over the board k is given by $\sum_{\ell=1}^{r} \sum_{i \in S \cap V_k} \bar{d}_i y_{\ell i} = q_k(S)$ since all the demand of S is served by the r routes. Now, let $\alpha_{\ell k}$ and $\beta_{\ell k}$ be the total line length drawn by pen ℓ over the white and the gray stripes of board k, respectively, for $k = 1, \ldots, s$, and $\ell = 1, \ldots, r$. We have that the total ink spent by each pen ℓ is given by

$$\begin{aligned}
&\sum_{k=1}^{s} (\alpha_{\ell k} + (1+\kappa)\beta_{\ell k}) = \sum_{k=1}^{s} ((\alpha_{\ell k} + \beta_{\ell k}) + \kappa \beta_{\ell k}) \\
&\leq \sum_{k=1}^{s} \left(\sum_{i \in S \cap V_k} \bar{d}_i y_{\ell i} + \kappa \min \left\{ \frac{b_k}{\kappa}, \sum_{i \in S \cap V_k} \bar{d}_i y_{\ell i} \right\} \right) \\
&\leq \sum_{k=1}^{s} \left(\sum_{i \in V_k} \bar{d}_i y_{\ell i} + \min \left\{ b_k, \sum_{i \in V_k} \kappa \bar{d}_i y_{\ell i} \right\} \right)
\end{aligned}$$

$$= \max_{d \in \mathcal{D}^{part}} \left\{ \sum_{i \in V^0} d_i y_{\ell i} \right\} \leq C$$

where the first inequality is a consequence of Proposition EC.3, and the last one holds because ℓ is a feasible route for the robust CVRP. Hence, the constructed solution is feasible for the SCP instance, finishing the proof. □

We are now able to prove the main result of this section.

Proof of Theorem 5 First, we show that γ_k is the exact line length drawn contiguously by a pen with ink C over the board k if it is used exclusively in this board. To see this, note that, for $C \leq \frac{1+\kappa}{\kappa} b_k$, where board k is completely gray, $\gamma_k = \frac{C}{1+\kappa}$ gives the exact length that can be drawn by a pen with ink C over a gray area. Otherwise, when $C > \frac{1+\kappa}{\kappa} b_k$, a pen with ink C spends $\frac{1+\kappa}{\kappa} b_k$ drawing a total length of $\frac{b_k}{\kappa}$ over the gray stripes, and the remaining ink to draw a total length of $C - \frac{1+\kappa}{\kappa} b_k$ over the white stripes. The sum of these lengths is exactly $\gamma_k = C - b_k$.

Now, note that $\left\lfloor \frac{q_k(S)}{\gamma_k} \right\rfloor$ is the number of times a pen becomes empty when crossing a board k (assuming that none of the pens used in this board is used elsewhere). Moreover, $\hat{q}_k(S)$ is the remaining height of board k after excluding the part crossed by these pens. Given that, the exact total ink required to cross board k can be expressed as

$$C \left\lfloor \frac{q_k(S)}{\gamma_k} \right\rfloor + \hat{q}_k(S) + \kappa \min \left\{ \frac{b_k}{\kappa}, \hat{q}_k(S) \right\},$$

for $k = 1 \ldots, s$. Thus, summing it up for all boards, dividing by C, and rounding the result up gives a lower bound on $r^*(S)$ which is exactly equal to $\hat{r}(S)$. Hence, by Proposition EC.4, $\hat{r}(S)$ is a valid lower bound on the left-hand side of (5) for any feasible robust CVRP solution. □

EC.1.8. Proof of Proposition 1

Note that, for the particular case considered here, $\tilde{r}(S)$ can be rewritten as

$$\left\lceil \frac{\sum_{k=1}^{s} (q_k(S) + \min\{b_k, \kappa\, q_k(S)\})}{C} \right\rceil,$$

and

$$\begin{aligned}\dot{r}(S) &= \sum_{k=1}^{s} \sum_{i \in S \cap V_k} \min_{\theta \in \{0, e_k\}} \frac{d_i^\theta}{C - b^\top \theta} \\ &= \sum_{k=1}^{s} \sum_{i \in S \cap V_k} \min \left\{ \frac{(1+\kappa)\bar{d}_i}{C}, \frac{\bar{d}_i}{C - b_k} \right\} \\ &= \sum_{k=1}^{s} \min \left\{ \frac{1+\kappa}{C}, \frac{1}{C - b_k} \right\} q_k(S) \\ &= \sum_{k=1}^{s} \frac{1}{C} \left(q_k(S) + \min \left\{ \kappa, \frac{b_k}{C - b_k} \right\} q_k(S) \right),\end{aligned}$$

where e_k represents a vector with the kth component equal to one, and all remaining ones equal to zero. The first equality holds because the minimum of $\frac{d_i^\theta}{C - b^\top \theta}$ over $\tilde{\Theta}$ (here assumed to be equal to Θ) is always achieved when $\theta_\ell = 0$ for all $\ell \neq k$. Hence, to prove that $\hat{r}(S) \geq \max\{\dot{r}(S), \tilde{r}(S)\}$, it is sufficient to show that

$$\begin{aligned}&C \left\lfloor \frac{q_k(S)}{\gamma_k} \right\rfloor + \hat{q}_k(S) + \min\{b_k, \kappa\, \hat{q}_k(S)\} \\ &\quad \geq \max \left\{ q_k(S) + \min\{b_k, \kappa\, q_k(S)\},\, q_k(S) + \min \left\{ \frac{b_k}{C - b_k}, \kappa \right\} q_k(S) \right\},\end{aligned}$$

or, equivalently, that

$$C \left\lfloor \frac{q_k(S)}{\gamma_k} \right\rfloor + \hat{q}_k(S) + \min\left\{b_k, \kappa\, \hat{q}_k(S)\right\} \geq q_k(S) + \min \left\{ \max \left\{ 1, \frac{q_k(S)}{C - b_k} \right\} b_k,\, \kappa\, q_k(S) \right\}, \quad \text{(EC.19)}$$

for $k = 1, \ldots, s$.

We divide the proof of (EC.19) into two cases. First, assume that $\frac{C}{1+\kappa} \geq C - b_k$. This implies that

$$\gamma_k = \frac{C}{1+\kappa}, \quad \text{(EC.20)}$$

and also that $\frac{b_k}{\kappa} \geq \frac{C}{1+\kappa} = \gamma_k$. Moreover, by definition of $\hat{q}_k(S)$, it is smaller than γ_k.

Hence, we have that

$$b_k > \kappa\, \hat{q}_k(S).$$

Applying this result, the definition of $\hat{q}_k(S)$, and (EC.20) to the lhs of (EC.19) gives the expression

$$C\left\lfloor \frac{q_k(S)}{\gamma_k} \right\rfloor + (1+\kappa)\left(q_k(S) - \frac{C}{1+\kappa}\left\lfloor \frac{q_k(S)}{\gamma_k} \right\rfloor \right) = (1+\kappa)q_k(S),$$

which is greater than or equal to the rhs of (EC.19).

Now, it remains to prove (EC.19) for the case where $\frac{C}{1+\kappa} < C - b_k = \gamma_k$, which implies that

$$C < (C - b_k) + \kappa\gamma_k$$

$$b_k < \kappa\,\gamma_k. \tag{EC.21}$$

In this case, we may rewrite the lhs of (EC.19) as

$$\begin{aligned} C\left\lfloor \frac{q_k(S)}{\gamma_k} \right\rfloor + q_k(S) - (C-b_k)\left\lfloor \frac{q_k(S)}{\gamma_k} \right\rfloor + \min\left\{ b_k, \kappa\, q_k(S) - \kappa\,\gamma_k \left\lfloor \frac{q_k(S)}{\gamma_k} \right\rfloor \right\} \\ = q_k(S) + \min\left\{ \left(\left\lfloor \frac{q_k(S)}{\gamma_k} \right\rfloor + 1 \right) b_k, \kappa\, q_k(S) + (b_k - \kappa\,\gamma_k)\left\lfloor \frac{q_k(S)}{\gamma_k} \right\rfloor \right\}, \end{aligned}$$

which can be shown to be greater than or equal to the rhs of (EC.19) by applying (EC.21).

To show that the inequality can be strict, we extend Example EC.3 by including the customers 5 and 6 in $S \cap V_2$, with $\bar{d}_5 = \bar{d}_6 = \hat{d}_5 = \bar{d}_6 = 2$. In this case, $\tilde{r}(S)$ remains equal to 2 because the deviation considered for partition 2 is already at its maximum, and the total demand to be served, including these deviations, increases from 7 to only $11 < 2C$. Moreover, $\dot{r}(S)$ increases by $\frac{d_5^{(0,1)}}{C-2} + \frac{d_6^{(0,1)}}{C-2} = 1$, becoming also equal to 2. However, $\hat{r}(S) = 3$ since $\gamma_2 = 4$, $q_2(S) = 8$, and $\hat{q}_1(S) = 1$.

□

EC.1.9. Proof of Proposition 2

It is enough to prove that there exists $\xi \in \Xi$ such that $\sum_{\ell=1}^{p} \hat{d}_{i_\ell}\xi_{i_\ell} + \sum_{\ell=q+1}^{|r'|} \hat{d}_{j_\ell}\xi_{j_\ell} = \tilde{d}(r'')$. For that, we use the fact that ξ^* is the worst-case scenario for both r and r'. Clearly, if $\Gamma_1 + \Gamma_2 \leq \Gamma$ the proposition holds since $\tilde{d}(r'') = \sum_{\ell=1}^{p} \hat{d}_{i_\ell}\xi^*_{i_\ell} + \sum_{\ell=q+1}^{|r'|} \hat{d}_{j_\ell}\xi^*_{j_\ell}$. Next, we prove that it also holds only for $\Gamma_1 + \Gamma_2 > \Gamma$ and $\tilde{d}_1 \geq \tilde{d}_2$, since the remaining case is analogous. For that, let

$$\dot{\xi}_\ell = \begin{cases} \frac{\Gamma - \Gamma_1}{\Gamma_2}\xi^*_\ell \text{ if } \ell \in \{j_{q+1}, \ldots, j_{|r'|}\} \\ \xi^*_\ell \qquad \text{otherwise.} \end{cases}$$

Clearly $\dot{\xi} \in \Xi$. Moreover, since $\sum_{\ell=q+1}^{|r'|} \hat{d}_{j_\ell}\dot{\xi}_{j_\ell} = (\Gamma - \Gamma_1) \sum_{\ell=q+1}^{|r'|} \frac{\hat{d}_{j_\ell}\xi^*_{j_\ell}}{\Gamma_2} = (\Gamma - \Gamma_1)\tilde{d}_2$, we have that $\sum_{\ell=1}^{p} \hat{d}_{i_\ell}\dot{\xi}_{i_\ell} + \sum_{\ell=q+1}^{|r'|} \hat{d}_{j_\ell}\dot{\xi}_{j_\ell} = \tilde{d}(r'')$, completing the proof. □

EC.2. Three examples for the new capacity cuts

To simplify the cut strength analysis that follows, we assume from now on that $\tilde{\Theta} = \Theta$. The first two examples look at the case $\mathcal{D} = \mathcal{D}^{card}$.

Example EC.1. Consider that $S = \{1, \ldots, 20\}$, $\Gamma = 1$, $C = 3$, and $\bar{d}_1 = \cdots = \bar{d}_{20} = \hat{d}_1 = \cdots = \hat{d}_{20} = 1$. In this case, since only one deviation is allowed for all $d \in \mathcal{D}$, we obtain that $\tilde{r}(S) = \lceil 21/3 \rceil = 7$. Alternatively, since $\tilde{\Theta} = \{0, 1\}$, we have that $\dot{r}(S) = 20 \min\{2/3, 1/2\} = 10$.

Although $\dot{r}(S)$ is usually much larger than $\tilde{r}(S)$ when the number of routes required to serve S is large, the next example shows that the opposite scenario may occur if only two routes are required.

Example EC.2. Consider $S = \{1, \ldots, 5\}$, $\Gamma = 3$, $C = 15$, $\bar{d}_1 = \hat{d}_1 = 5$, and $\bar{d}_2 = \cdots = \bar{d}_5 = \hat{d}_2 = \cdots = \hat{d}_5 = 1$. In this case, since the total demand to be served in S can reach $16 > C$ (by deviating d_1, d_2, and d_3, for example), we obtain that $\tilde{r}(S) = 2$. However, since $\tilde{\Theta} = \{0, 1\}$, we have that $\dot{r}(S) = \min\{10/15, 9/12\} + 4 \min\{2/15, 1/12\} = 1$.

Note that Example EC.1 can be easily adapted for $\mathcal{D} = \mathcal{D}^{part}$ because all deviations are unitary. For that, it is enough to assume that all customers in S belong to the same partition V_k of V^0, and that $b_k = \Gamma = 1$. This shows that $\dot{r}(S)$ can also be strictly larger than $\tilde{r}(S)$ for the uncertainty set proposed in Gounaris et al. (2013). It is worth mentioning that all deviations in this example are proportional to the corresponding nominal demand values, which is an assumption of the special case addressed by Theorem 5. The third example shows that the opposite strict inequality may also occur regardless of whether deviations are proportional to nominal values or not.

Example EC.3. In this case, assume that V^0 is partitioned into two sets ($s = 2$), $S = \{1, 2, 3, 4\}$, and $S \cap V_1 = \{1\}$. Moreover, we have $C = 6$, $\bar{d}_1 = \cdots = \bar{d}_4 = \hat{d}_1 = \cdots = \hat{d}_4 = 1$, and $b_1 = b_2 = 2$. In this case, note that $\tilde{r}(S) = 2$ since the total deviation of d_2, d_3, and d_4 can reach the limit of the

partition 2, and d_1 can deviate by one unit since it is in another partition, resulting in a total demand of $7 > C$ units to be served. However, since $\tilde{\Theta} = \{(0,0),(0,1),(1,0),(1,1)\}$, we have

$$\dot{r}(S) = \frac{d_1^{(1,0)}}{C-2} + \frac{d_2^{(0,1)}}{C-2} + \frac{d_3^{(0,1)}}{C-2} + \frac{d_4^{(0,1)}}{C-2} = 1.$$

EC.3. Further algorithmic details

EC.3.1. Branch-cut-and-price outline

In the algorithm, the linear relaxation of the formulation (14)–(17) is solved by column generation, stabilized using the automatic dual price smoothing technique by Pessoa et al. (2018). To accelerate the solution of each pricing subproblem $\theta \in \tilde{\Theta}$ we use the ng-path relaxation (Baldacci et al. 2011) of R^θ. This relaxation includes non-elementary routes, i.e. that may pass by the same customer more than once. The ng-path relaxation is dynamically adjusted using the approach of Bulhoes et al. (2018).

The pricing problems are solved using the bi-directional bucket graph based labelling algorithm proposed by Sadykov et al. (2017). In it, each label represents a partial path started at the depot. Labels are grouped into buckets based on their final vertices and on ranges defined for the accumulated demand. As d^θ is continuous in general, such bucket definition has an advantage in our setting over a more traditional way based on resource discretisation, used for example in Pecin et al. (2017b). A bucket arc exists between a pair of buckets if a label in the first bucket can be extended to a label in the second one. The bucket graph (which consists of buckets and bucket arcs) is useful because it helps to determine an efficient order for label extensions. Additionally, the bucket graph is used to avoid label extensions that are proved not to contribute to a solution that improves the current best one. This is performed by removing bucket arcs from the bucket graph based on a reduced cost argument, as in (Sadykov et al. 2017).

We separate capacity cuts which are specific for the robust CVRP and which are presented below in Section 4. We also separate generic rank-1 Chvatal-Gomory cuts for up to 5 rows (Pecin et al. 2017a). The limited memory technique by Pecin et al. (2017b) is used to decrease the negative

impact of rank-1 cuts on the difficulty of the pricing subproblems. Strong branching on edge variables is performed as in Pecin et al. (2017b). The elementary route enumeration procedure proposed by Baldacci et al. (2008) is employed to enumerate routes with reduced costs smaller that the current primal-dual gap. If the number of enumerated routes is small enough, the current branch-and-bound node is solved by the CPLEX MIP solver.

EC.3.2. Separation of capacity cuts

Let $\bar{x}$ be a fractional solution to RVRP-2IF. We have both types of separation procedures: one specialized in the separation of (20), and another one that separates the weaker inequalities (19) using the procedure of Lysgaard et al. (2004).

We separate robust capacity inequalities (20) at each node of the branch-and-bound tree using the heuristic described in Algorithm 1, which is based on the separation heuristic used in Uchoa et al. (2008). In this algorithm, the limit on the number of inserted cuts is set to 500.

Moreover, we use the procedure of Lysgaard et al. (2004) to separate the weaker version (19) obtained by replacing its right-hand side with $\lceil \dot{r}(S) \rceil = \lceil \sum_{i \in S} \dot{d}_i / \dot{C} \rceil$ where $\dot{d}_i = \min_{\theta \in \tilde{\Theta}} \{ d_i^\theta / (C - b^\top \theta) \}$ and $\dot{C} = 1$. Note that this is the exact expression for the right-hand side of the rounded capacity cuts separated by Lysgaard et al. (2004) with $\dot{d}_i$ and $\dot{C}$ replacing $\bar{d}_i$ and C, respectively. Since the available implementation of this separation procedure requires that all demands and the vehicle capacity are integer, we multiply them by a large scale factor and round them properly to ensure the validity of the cuts.

EC.3.3. Speeding-up the search over inter-route neighborhoods

In Algorithm 2, lines 2-5 implement the search in the two intra-route neighborhoods, where the incumbent solution is updated upon every found improvement. Inter-route neighborhoods are tried only after no more intra-route change can be made. Lines 7-21 and 22-31 implement the search in the 2-OPT*and the insert neighborhoods, respectively. For the 2-OPT*, since the change is symmetric, if the pair of routes (r, r') is tried in line 7, (r', r) is not tried. However, the pair (r, the reverse of r') is also tried. In this case, the proposed mechanism to avoid trying useless changes

Algorithm 1: Separation heuristic for inequalities (20) or (5)

for $i \in V^0$ **do**
  $S_i := \{i\}$;
  repeat
    Add to S_i the node $j \in V^0 \setminus S_i$ that leads to the largest cut violation (or smallest slack) and results in a set not generated so far;
    Check if S_i leads to a violation;
    if *the number of violated cuts found reaches the limit* **then**
      return *All violated cuts found*
  until *no such node j exists*;
return *All violated cuts found*

uses the fact that, if a modified route is infeasible, the same route with one additional customer is still infeasible. This is done in lines 13 and 19 for route r, and lines 15 and 20 for route r'. A similar mechanism is implemented for the insert neighborhood, where an insertion that causes infeasibility will make the route infeasible regardless of the insertion position. This is implemented in lines 27 and 30, which avoid trying to insert the same customer in other positions in this case.

EC.4. Instance generation

Here, we precisely describe the generation of the uncertainty set data for the new benchmark set proposed for $\mathcal{D}^{card}$. Given a deterministic CVRP instance and parameters μ, ρ and τ for a given configuration, the full specification of $\mathcal{D}^{card}$ is computed as follows. Note that n is defined here as the number of customers, not including the depot.

1. The nominal demand vector $\bar{d}$ is identical to the deterministic demand vector d of the original instance.
2. $\hat{d} = \mu\bar{d}$.
3. $\Gamma = \left\lfloor \frac{\rho n}{m} \right\rfloor$.
4. This last step is more involved since it aims to define a modified value for the vehicle capacity C ensuring that the resulting instance is feasible and the capacity is not too loose (otherwise

Algorithm 2: Local Search (parameter: an incumbent solution INC)

```
repeat
    for each possible 2-OPT move over INC do
        if it improves INC then replace INC by the new solution
    for each possible reinsertion move over INC do
        if it improves INC then replace INC by the new solution
    if INC was not changed in the current iteration then
        for each pair of routes r and r' in INC do
            for p = 0, ..., |r| do
                q_0 ← 0;
                for q = q_0, ..., |r'| do
                    try exchanging the last |r| − p customers of r with the last |r'| − q
                     customers of r';
                    if r fails in the approximate feasibility test then
                        q_0 ← q + 1; continue for;
                    if r' fails in the approximate feasibility test then
                        exit for;
                    if it improves the cost of INC then
                        if INC fails in the exact feasibility test then
                            if INC failed because of r then
                                q_0 ← q + 1; continue for;
                            else exit for;
                        else replace INC by the new solution
        for each pair of routes r and r' in INC do
            for p = 1, ..., |r| do
                for q = 0, ..., |r'| do
                    try inserting the pth customer of r after q customers in r';
                    if r' fails in the approximate feasibility test then
                        exit for;
                    if it improves the cost of INC then
                        if r' fails in the exact feasibility test then
                            exit for;
                        else replace INC by the new solution
until INC does not change in the current iteration;
```

using a smaller number of vehicles would be desirable in practice). For that, we define a function BP(c) that receives a tentative capacity value c and computes an upper approximation of the minimum number of vehicles required to make the current robust CVRP instance feasible with c as the vehicle capacity. The algorithm used to evaluate BP is detailed later. Then, we set $C =$

$\lfloor \tau C_{\max} + (1-\tau)C_{\min} \rfloor$, where $C_{\min} = \min\{c \in \mathbb{N} \mid \text{BP}(c) \leq m\}$ and $C_{\max} = \min\{c \in \mathbb{N} \mid \text{BP}(c) \leq m-1\}$.

First, we remark that function BP(c) can be fulfilled by any heuristic for the robust counterpart of the Bin Packing Problem (BPP). To see this, note that BP ignores the objective function of the robust CVRP instance being processed and tries to pack the customer into the minimum number of identical vehicles with capacity c. Thus, we compute BP using the well-known first-fit decreasing heuristic for the deterministic version of BPP, where customers are ordered in a non-increasing order by the sum of their maximum demands allowed by the uncertainty set. At each iteration, the heuristic searches in the ordered list of customers for the first one that fits into the current vehicle. Whenever no customers can be inserted in the current vehicle, a new vehicle is inserted in the solution. Although this method is not guaranteed to compute the minimum number of vehicles required, we observed that instances created with $\tau = 0$ were not realistic since their solution costs (now considering the CVRP objective function) usually increased by large factors with respect to the deterministic version of the problem. Thus, we decided to restrict our attention to instances with $\tau \geq 1.5$. For the sake of easy reproducibility of our results, we report the values of $C_{\min}$ and $C_{\max}$ for all instances of the proposed benchmark set in Subsection EC.6.1.

EC.5. Detailed numerical experiments

EC.5.1. Effect of preprocessing

EC.5.1.1. Uncertainty set $\mathcal{D}^{part}$ Table EC.1 shows the effect of the preprocessing technique introduced in Subsection 2.3 based on Lemma 3 for $\mathcal{D}^{part}$. In this table, the last 4 columns show the average number of vehicles (m), the average number of subproblems after preprocessing (#sp), the percentage reduction (%red.) obtained with respect to the initial number of subproblems, which is always equal to $2^s = 16$, and the number of instances that could be solved as deterministic CVRP because only one subproblem remained.

From Table EC.1, it can be seen that the proposed preprocessing method is very effective for the literature instances. Almost 80% of the subproblems have been removed, and 22 of 90 instances were solved as deterministic CVRP. Moreover, the preprocessing method seems to be more effective

Table EC.1 Effect of preprocessing for $\mathcal{D}^{part}$

In. cls	#in.	m	#sp	%red.	#det.
A	26	7.1	2.7	83.4%	7
B	23	7.2	3.9	75.8%	0
E	11	7.3	3.6	77.3%	4
F	3	5.0	5.0	68.8%	0
M	3	9.7	1.3	91.7%	2
P	24	7.3	4.3	73.2%	9
all	90	7.2	3.6	77.8%	22

for instance classes where the average number of vehicles is larger. We believe that this is not a coincidence and that the way instances have been generated favors the observed reduction. Recall that the limit on the total demand deviation for each quadrant is fixed as 75% of the sum of demand deviations. Since each quadrant has roughly 25% of the total demand to be served and deviations are proportional to nominal demand values, the limit imposed to the total demand deviation can only be reached for a route that serves roughly 18.75% ($> 1/6$) of the total demand. Thus, if the number of vehicles is much larger than 6, the preprocessing step is likely to prove that the total deviation limit cannot be reached for many quadrants. This hypothesis is confirmed by the chart of Figure EC.2, where each point represents one or more instances whose coordinates are the number of vehicles and the number of remaining subproblems after preprocessing. The decrease on the number of subproblems as the number of vehicles increases is very clear.

Although the previous observation has been caused by a specific artificial property of the benchmark set, we believe that similar situations may occur in real-life applications, leading to impressive reductions on the number of subproblems. For testing robust optimization algorithms however, it is now desirable that the new benchmark sets are designed to avoid the existence of redundant constraints in the uncertainty set description. This is the case for the new benchmark set proposed in Subsection 6.2.1.

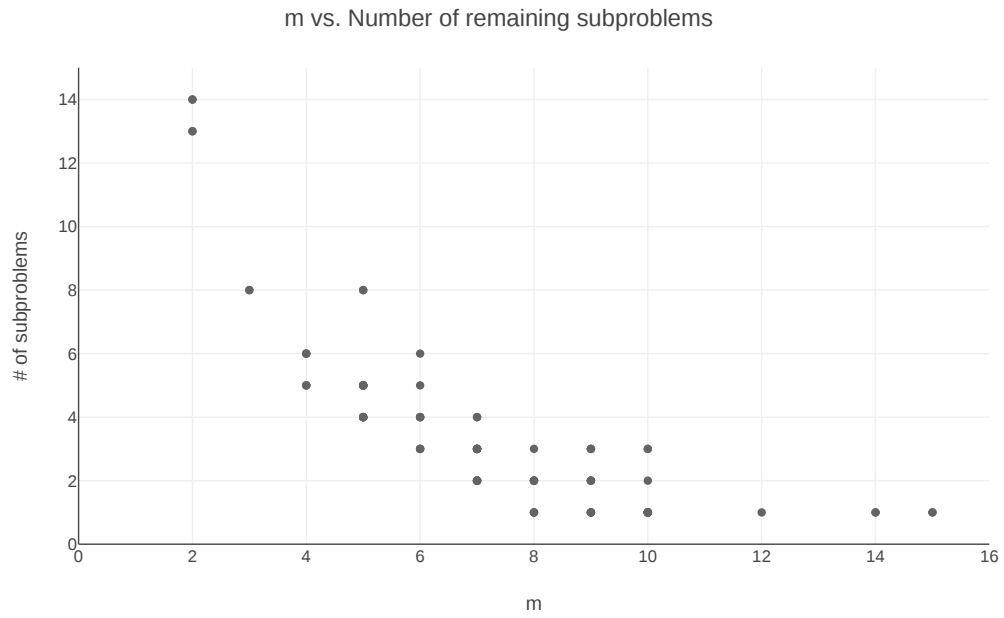

Figure EC.2 **Relation between the number of vehicles and the number of subproblems remaining after preprocessing.**

EC.5.1.2. Uncertainty set $\mathcal{D}^{card}$ Table EC.2 presents a measure of the effect of preprocessing the subproblems. In this table, the first seven rows after the headers refer to the main configuration described in the previous subsection, containing results for each instance class separately, and then aggregated results. The additional six rows provide aggregated results for all instance classes considering the remaining configurations. The results in these rows should be compared with that in the seventh row. The first two columns contain the instance class or configuration identifier (In. cls), and the number of instances in that subset (#in.). Tables 4, EC.4, and EC.3 follow the same format except that results for configurations other than the main one are not presented in the last two tables. The last four columns of Table EC.2 contain the average number of distinct demand values (#dem.), the average number of subproblems without preprocessing (#sp lit.) according to Theorem 2, and the average number of subproblems after preprocessing(#sp new), and the percentage reduction (%red.).

From Table EC.2, we observe that the effect of preprocessing is not so expressive but still significant for the new benchmark instances. This was expected since the instances have been

Table EC.2 Effect of preprocessing for $\mathcal{D}^{card}$

In. cls	#in.	#dem.	#sp lit.	#sp new	%red.
A	27	20.7	16.6	13.7	16.7%
B	23	21.6	16.9	14.0	16.9%
E	13	24.3	17.4	14.1	16.0%
F	2	53.5	24.5	21.5	11.9%
M	2	14.0	10.5	8.5	26.3%
P	23	25.5	18.3	16.2	9.4%
all	90	22.7	17.0	14.4	14.7%
Low $\hat{d}$	90	22.7	17.0	14.8	12.4%
High $\hat{d}$	90	22.7	17.0	14.1	16.1%
Low Γ	90	22.7	17.8	17.7	0.8%
High Γ	90	22.7	16.1	10.6	32.6%
Low C	90	22.7	17.0	14.2	16.0%
High C	90	22.7	17.0	14.9	11.6%

generated in a way that Γ is never larger than the average route length. We also observe that the effect of preprocessing increases for larger values of Γ, and that Theorem 2 provides an important reduction on the number of subproblems with respect to the number of distinct demand values but it is far away from dividing it by two because most instances have a large number of customers with the same associated demand.

EC.5.2. Effect of new capacity cuts

The aim of this subsection is to present a measure of the effect of the strengthened robust capacity cuts introduced in Subsection 4 for the generic uncertainty set $\mathcal{D}$, and its specific version given by Theorem 5 for $\mathcal{D}^{part}$ assuming demand deviations proportional to the corresponding nominal demand value. The results presented in this table were obtained in a run of BCP only for the root

node, with all other cuts, fixing by reduced cost and enumeration of useful elementary routes disabled. We compare two runs. In the first one, only the capacity inequalities proposed by Gounaris et al. (2013) are separated using the procedure described in Section EC.3.2 of the electronic companion. The second one separates the new cuts using both this procedure and the one proposed by Lysgaard et al. (2004) for the deterministic CVRP. In the second case, the separation algorithm receives modified demands described in Subsection 4, and the violated cuts found are replaced by the strongest available ones, which are the specific version for $\mathcal{D}^{part}$ and the more generic version for $\mathcal{D}^{card}$. For $\mathcal{D}^{card}$, we considered only the main configuration.

Table EC.3 presents the obtained results. In this table, the columns labeled by "#in." report the number of instances considered in each row, which are different for $\mathcal{D}^{part}$ and $\mathcal{D}^{card}$. These numbers may be smaller than in the previous tables because we disregard all instances for which the gap left by the pure column generation lower bound is zero. The columns labeled by "cl. gap" and "gap rd." show the averages of the percentage gap closed by the literature cuts and the percentage reduction of the gap obtained by replacing the literature cuts with the newly proposed strengthened cuts. Let 1stLB, litLB, and newLB be the root lower bounds obtained by BCP without any cut, with literature cuts only, and with the new cuts. Let also UB be the best known solution cost. The percentage gap closed by the literature cuts and the percentage gap reduction obtained with the new cuts are given by $\frac{\text{litLB}-\text{1stLB}}{\text{UB}-\text{1stLB}} \times 100\%$ and $\frac{\text{newLB}-\text{litLB}}{\text{UB}-\text{litLB}} \times 100\%$, respectively. Because of that, the instances for which the gap left by the literature cuts is zero are disregarded in the columns under the header "New cuts". The remaining six columns show two additional measures for each run of each benchmark set: the number of closed instances, i.e. that with final gap zero, labeled by "#cl.", and the average number of cut rounds needed, labeled by "#c.r.".

Overall, Table EC.3 shows that the literature cuts are very effective for $\mathcal{D}^{part}$ as they close more than 60% of the gap, and that the new cuts close 33% of the remaining gap, which is a significant improvement. However, the performance of the new cuts is highly dependent on the instance class. For example, it closes almost 80% of the remaining gap for the class M and more than 50% for the

Table EC.3 Effect of the new capacity cuts

In.	$\mathcal{D}^{part}$							$\mathcal{D}^{card}$						
		Lit. cuts			New cuts				Lit. cuts			New cuts		
cls	#in.	cl. gap	#cl.	#c.r.	gap rd.	#cl.	#c.r.	#in.	cl. gap	#cl.	#c.r.	gap rd.	#cl.	#c.r.
A	25	55.9%	1	2.8	36.2%	0	2.9	27	33.4%	0	2.7	37.9%	0	2.9
B	23	81.4%	5	2.7	51.5%	8	2.8	23	53.3%	0	2.7	64.5%	0	2.9
E	11	45.7%	2	2.5	9.3%	2	2.5	13	38.2%	3	1.8	25.3%	4	2.2
F	2	91.6%	1	1.5	58.7%	1	2	2	43.5%	0	1	-14.6%	0	2
M	2	68.8%	0	2.5	77.6%	1	3	2	67.5%	0	3	27.2%	0	3
P	22	51.4%	4	2.3	17.6%	5	2.3	22	32.2%	2	2.1	17.6%	2	2.8
all	85	61.5%	13	2.6	33.5%	17	2.6	89	39.9%	5	2.4	37.3%	6	2.7

classes B and F. Moreover, the number of instances with gap zero increases from 13 to 17 with the new cuts. It is also clear that a small number of cut rounds are required for convergence in both cases. For $\mathcal{D}^{card}$, we note that the gap zero is obtained for less instances (only 5 with the literature cuts and 6 with the new cuts), and the literature cuts are less effective in general, closing roughly 40% of the column generation gap only. From that gap, the new cuts close more than 37% in the average, again with a large variation from one instance class to the other. For example, for the class B, which is the hardest one for BCP, the gaps closed by both the literature cuts and the new cuts are much larger than for other classes. This suggests that further improving these cuts may be a way to solve the instances left open by this work. However, for the class F, the new cuts provided lower bounds that are worse in the average than that of the literature cuts. This is only possible because the cut separation routine used is not exact. In fact, this happened only for the instance F-n45-k4, where the literature cuts closed 87.1% of the initial gap and the new cuts closed only 81.4% of this initial gap, resulting in a gap 43.4% larger than the gap left by the literature cuts.

EC.5.3. Effect of approximate feasibility checking for $\mathcal{D}^{card}$

Table EC.4 compares the runtimes of ILS-VNS with and without performing approximate feasibility checks, for $\mathcal{D}^{card}$. The last three columns of this table contain the mean runtimes performing these checks (app.t.time), the mean runtimes not performing them, i.e. performing only exact checks (ex.t.time), and the average ratio between the time spent not performing the checks and the time spent performing them (ex.app.ratio).

Table EC.4 Effect of the approximate feasibility testing for $\mathcal{D}^{card}$

In. cls	# in.	app.t. time	ex.t. time	ex.app. ratio
A	27	1.98	5.82	2.96
B	23	2.57	7.09	2.78
E	13	2.85	6.79	2.47
F	2	1.26	2.07	1.66
M	2	5.72	21.04	3.68
P	23	1.93	4.47	2.47
all	90	2.25	5.88	2.70

EC.6. Raw data for Reproducibility

EC.6.1. Capacity ranges for the new benchmark set

Table EC.5: Minimum and maximum capacities for $\mathcal{D}^{card}$

Inst.	C_{min}	C_{max}	Inst.	C_{min}	C_{max}	Inst.	C_{min}	C_{max}
A-n32-k5	104	126	B-n38-k6	108	126	E-n76-k14	123	132
A-n33-k5	111	135	B-n39-k5	111	135	E-n101-k8	228	258
A-n33-k6	115	134	B-n41-k6	120	141	E-n101-k14	130	140
A-n34-k5	116	139	B-n43-k6	110	129	F-n45-k4	2275	3019

A-n36-k5	112	137	B-n44-k7	115	132	F-n72-k4	36382	48097
A-n37-k5	104	128	B-n45-k5	124	151	M-n101-k10	231	251
A-n37-k6	119	140	B-n45-k6	124	146	M-n121-k7	244	280
A-n38-k5	121	148	B-n50-k7	110	127	P-n19-k2	194	358
A-n39-k5	121	148	B-n50-k8	116	129	P-n20-k2	196	363
A-n39-k6	110	129	B-n51-k7	123	141	P-n21-k2	186	347
A-n44-k6	120	141	B-n52-k7	109	125	P-n22-k2	193	357
A-n45-k6	125	147	B-n56-k7	110	126	P-n22-k8	3420	3790
A-n45-k7	114	129	B-n57-k7	127	145	P-n23-k8	50	57
A-n46-k7	108	123	B-n57-k9	112	124	P-n40-k5	155	188
A-n48-k7	114	130	B-n63-k10	116	127	P-n45-k5	173	210
A-n53-k7	121	140	B-n64-k9	124	137	P-n50-k7	170	195
A-n54-k7	121	138	B-n66-k9	121	134	P-n50-k8	148	166
A-n55-k9	116	129	B-n67-k10	114	124	P-n50-k10	117	128
A-n60-k9	115	128	B-n68-k9	117	130	P-n51-k10	96	106
A-n61-k9	124	138	B-n78-k10	119	130	P-n55-k7	184	209
A-n62-k8	116	131	E-n13-k4	5820	7420	P-n55-k8	164	184
A-n63-k9	124	138	E-n22-k4	6940	9000	P-n55-k10	131	143
A-n63-k10	117	129	E-n23-k3	5330	6266	P-n55-k15	85	90
A-n64-k9	120	133	E-n30-k3	5330	7865	P-n60-k10	141	155
A-n65-k9	123	137	E-n31-k7	163	190	P-n60-k15	91	96
A-n69-k9	118	131	E-n33-k4	9260	12129	P-n65-k10	150	165
A-n80-k10	118	130	E-n51-k5	194	237	P-n70-k10	164	181
B-n31-k5	103	126	E-n76-k7	245	280	P-n76-k4	427	553
B-n34-k5	115	141	E-n76-k8	214	241	P-n76-k5	341	416

B-n35-k5	111	137	E-n76-k10	170	186	P-n101-k4	457	594

EC.6.2. Raw ILS-VNS results for $\mathcal{D}^{part}$

Inst.	UB	avg t.	min t.	max t.	Inst.	UB	avg t.	min t.	max t.
A-n32-k5	748	0.30	0.30	0.31	B-n66-k9	1251	2.75	0.93	6.49
A-n33-k5	642	0.28	0.24	0.31	B-n67-k10	1007	1.15	1.04	1.61
A-n33-k6	717	0.30	0.26	0.55	B-n68-k9	1205	31.25	1.84	112.23
A-n34-k5	715	0.32	0.29	0.38	B-n78-k10	1131	6.57	1.29	20.89
A-n36-k5	755	0.40	0.30	0.64	E-n22-k4	373	0.14	0.14	0.14
A-n37-k5	650	0.41	0.37	0.45	E-n23-k3	563	0.29	0.22	0.52
A-n37-k6	892	0.31	0.30	0.33	E-n30-k3	475	0.29	0.28	0.29
A-n38-k5	704	1.20	0.40	3.84	E-n33-k4	814	0.37	0.37	0.37
A-n39-k5	777	0.64	0.37	1.36	E-n51-k5	516	0.84	0.81	0.88
A-n39-k6	787	0.40	0.38	0.49	E-n76-k7	661	4.20	1.56	8.87
A-n44-k6	909	2.35	0.60	4.32	E-n76-k8	709	7.30	1.43	13.69
A-n45-k6	896	2.50	1.42	4.52	E-n76-k10	796	42.78	5.95	173.49
A-n46-k7	888	0.62	0.53	1.04	E-n76-k14	952	1.78	0.93	3.50
A-n48-k7	1033	0.63	0.53	0.96	E-n101-k8	789	8.90	2.93	21.58
A-n53-k7	974	0.71	0.59	0.93	E-n101-k14	1011	7.40	1.98	16.40
A-n54-k7	1106	2.32	0.52	7.68	F-n45-k4	718	0.85	0.64	1.18
A-n55-k9	1030	3.68	1.49	8.98	F-n72-k4	232	2.10	2.04	2.20
A-n60-k9	1280	1.66	0.86	4.14	F-n135-k7	1122	112.18	30.99	428.40
A-n61-k9	983	87.32	1.74	309.07	M-n101-k10	809	2.97	2.84	3.34
A-n62-k8	1219	4.29	1.05	10.08	M-n121-k7	994	6.83	3.11	13.04
A-n63-k9	1505	7.75	1.66	14.44	M-n151-k12	987	921.55	35.81	2416.68
A-n63-k10	1244	3.34	1.36	7.73	P-n16-k8	439	0.05	0.05	0.05

A-n64-k9	1326	2.78	0.89	5.08	P-n19-k2	195	0.12	0.12	0.12
A-n65-k9	1106	4.85	1.28	13.12	P-n20-k2	208	0.15	0.15	0.15
A-n69-k9	1109	7.13	1.71	12.66	P-n21-k2	208	0.17	0.16	0.17
A-n80-k10	1662	16.17	3.48	38.97	P-n22-k2	213	0.17	0.17	0.17
B-n31-k5	651	0.25	0.24	0.28	P-n22-k8	537	0.09	0.09	0.09
B-n34-k5	768	0.31	0.30	0.31	P-n23-k8	504	0.14	0.09	0.30
B-n35-k5	883	0.31	0.26	0.37	P-n40-k5	447	0.60	0.41	1.15
B-n38-k6	729	0.39	0.38	0.39	P-n45-k5	501	0.64	0.60	0.67
B-n39-k5	532	0.42	0.39	0.52	P-n50-k7	539	2.43	0.59	7.15
B-n41-k6	796	0.39	0.35	0.50	P-n50-k8	592	0.60	0.45	0.97
B-n43-k6	681	0.49	0.47	0.52	P-n50-k10	656	0.58	0.43	0.90
B-n44-k7	835	0.37	0.35	0.38	P-n51-k10	707	1.58	0.82	2.98
B-n45-k5	701	0.56	0.55	0.58	P-n55-k7	549	2.27	0.74	5.54
B-n45-k6	660	0.51	0.44	0.89	P-n55-k8	572	1.24	0.69	2.67
B-n50-k7	679	0.73	0.66	0.97	P-n55-k10	670	1.59	0.60	2.56
B-n50-k8	1224	5.97	0.98	15.52	P-n55-k15	889	1.04	0.48	2.17
B-n51-k7	961	2.85	0.66	7.22	P-n60-k10	712	0.82	0.65	1.95
B-n52-k7	675	0.88	0.71	1.32	P-n60-k15	931	26.82	2.50	74.61
B-n56-k7	623	0.78	0.76	0.80	P-n65-k10	765	8.40	1.33	21.81
B-n57-k7	1055	0.86	0.67	1.27	P-n70-k10	785	2.59	0.71	6.69
B-n57-k9	1540	25.60	2.42	67.59	P-n76-k4	590	3.75	2.45	6.01
B-n63-k10	1407	3.05	0.60	7.17	P-n76-k5	616	3.64	1.94	8.64
B-n64-k9	803	0.93	0.90	0.99	P-n101-k4	673	5.43	4.60	7.08

EC.6.3. Raw BCP results for $\mathcal{D}^{part}$

Inst.	root LB	UB	time	Inst.	root LB	UB	time

A-n32-k5	748.0	748	0.42	B-n66-k9	1249.2	1251	47.11
A-n33-k5	630.7	642	2.65	B-n67-k10	1006.0	1007	13.03
A-n33-k6	705.7	717	0.60	B-n68-k9	1204.1	1205	24.46
A-n34-k5	708.8	715	0.60	B-n78-k10	1130.3	1131	24.73
A-n36-k5	742.0	755	1.46	E-n22-k4	362.5	373	1.75
A-n37-k5	645.4	650	1.96	E-n23-k3	550.3	563	8.23
A-n37-k6	881.0	892	0.72	E-n30-k3	475.0	475	19.62
A-n38-k5	698.5	704	1.37	E-n33-k4	807.3	814	35.91
A-n39-k5	775.2	777	1.87	E-n51-k5	515.0	516	5.44
A-n39-k6	777.3	787	0.81	E-n76-k7	660.2	661	20.89
A-n44-k6	902.5	909	2.99	E-n76-k8	707.5	709	12.72
A-n45-k6	894.2	896	1.82	E-n76-k10	793.7	796	8.54
A-n46-k7	885.0	888	2.68	E-n76-k14	947.6	952	2.03
A-n48-k7	1026.4	1033	4.78	E-n101-k8	788.7	789	232.46
A-n53-k7	972.0	974	12.01	E-n101-k14	1011.0	1011	7.16
A-n54-k7	1105.5	1106	7.70	F-n45-k4	715.1	718	38.41
A-n55-k9	1023.8	1030	1.89	F-n72-k4	232.0	232	173.85
A-n60-k9	1276.2	1280	4.65	F-n135-k7	1111.8	1122	86700.00
A-n61-k9	978.4	983	5.28	M-n101-k10	806.3	809	3.18
A-n62-k8	1202.6	1214	15.46	M-n121-k7	993.4	994	163.50
A-n63-k9	1503.1	1505	4.79	M-n151-k12	979.1	985	6949.66
A-n63-k10	1233.0	1233	14.47	P-n16-k8	434.5	439	0.02
A-n64-k9	1321.8	1325	16.45	P-n19-k2	195.0	195	0.63
A-n65-k9	1101.8	1106	1.09	P-n20-k2	207.8	208	0.61
A-n69-k9	1105.5	1109	8.75	P-n21-k2	207.3	208	1.14

A-n80-k10	1659.1	1662	13.68	P-n22-k2	209.9	213	1.21
B-n31-k5	649.8	651	0.90	P-n22-k8	537.0	537	0.13
B-n34-k5	768.0	768	10.43	P-n23-k8	500.8	504	0.04
B-n35-k5	883.0	883	1.51	P-n40-k5	442.2	447	1.18
B-n38-k6	728.3	729	1.16	P-n45-k5	496.7	501	4.73
B-n39-k5	532.0	532	9.64	P-n50-k7	535.0	539	2.47
B-n41-k6	793.9	796	4.29	P-n50-k8	586.8	592	0.34
B-n43-k6	678.7	681	4.36	P-n50-k10	650.7	656	0.24
B-n44-k7	833.7	835	1.51	P-n51-k10	698.7	707	0.42
B-n45-k5	698.5	701	16.32	P-n55-k7	546.4	549	5.44
B-n45-k6	656.9	660	5.50	P-n55-k8	569.1	572	6.43
B-n50-k7	679.0	679	2.40	P-n55-k10	666.3	670	3.48
B-n50-k8	1222.5	1224	5.35	P-n55-k15	880.8	889	0.20
B-n51-k7	956.9	961	5.57	P-n60-k10	707.0	712	1.36
B-n52-k7	672.0	675	7.88	P-n60-k15	922.8	931	0.71
B-n56-k7	622.1	623	6.76	P-n65-k10	761.9	765	4.06
B-n57-k7	1052.9	1055	7.99	P-n70-k10	782.4	785	1.44
B-n57-k9	1539.1	1540	4.62	P-n76-k4	589.4	590	98.61
B-n63-k10	1407.0	1407	5.40	P-n76-k5	615.4	616	73.24
B-n64-k9	801.4	803	6.45	P-n101-k4	672.7	673	373.37

* Root LB value corresponds to gap 1 value on Table 2.

** Only underlined UB values are not proved to be optimal.

EC.6.4. Raw ILS-VNS results for $\mathcal{D}^{card}$

Inst.	UB	avg t.	min t.	max t.	Inst.	UB	avg t.	min t.	max t.

A-n32-k5	857	0.27	0.24	0.29	B-n64-k9	865	260.78	38.08	976.54
A-n33-k5	675	0.27	0.25	0.34	B-n66-k9	1319	4.14	1.62	10.42
A-n33-k6	758	0.42	0.25	1.09	B-n67-k10	1086	1.13	0.63	1.68
A-n34-k5	776	0.29	0.28	0.31	B-n68-k9	1298	20.30	2.50	69.54
A-n36-k5	823	0.42	0.30	0.79	B-n78-k10	1261	1305.63	157.17	3065.41
A-n37-k5	706	0.38	0.36	0.40	E-n13-k4	277	0.02	0.02	0.02
A-n37-k6	948	2.76	0.69	9.44	E-n22-k4	373	0.13	0.12	0.13
A-n38-k5	714	0.37	0.36	0.40	E-n23-k3	570	0.23	0.23	0.23
A-n39-k5	818	0.88	0.40	1.74	E-n30-k3	495	0.33	0.32	0.34
A-n39-k6	850	0.63	0.35	0.92	E-n31-k7	379	0.21	0.17	0.23
A-n44-k6	930	0.55	0.45	0.93	E-n33-k4	836	0.37	0.35	0.42
A-n45-k6	918	1.44	0.46	6.10	E-n51-k5	519	1.32	0.69	2.92
A-n45-k7	1163	8.31	0.55	29.40	E-n76-k7	699	5.07	1.85	11.90
A-n46-k7	988	0.52	0.39	0.84	E-n76-k8	736	11.34	1.93	29.46
A-n48-k7	1129	2.91	0.52	9.89	E-n76-k10	830	385.70	66.56	895.89
A-n53-k7	1019	1.91	0.99	4.47	E-n76-k14	1022	171.57	61.57	421.72
A-n54-k7	1169	3.41	0.77	8.77	E-n101-k8	826	25.06	3.41	81.78
A-n55-k9	1107	2.72	1.09	7.46	E-n101-k14	1121	419.22	6.58	1557.43
A-n60-k9	1408	6.62	2.45	12.19	F-n45-k4	736	0.74	0.72	0.78
A-n61-k9	1022	2.55	0.89	4.76	F-n72-k4	236	2.13	2.00	2.26
A-n62-k8	1339	9.73	3.11	18.01	M-n101-k10	918	3.87	1.80	7.70
A-n63-k9	1620	7.85	1.44	23.39	M-n121-k7	1030	8.47	4.58	14.39
A-n63-k10	1348	9.87	1.77	26.70	P-n19-k2	195	0.14	0.14	0.15
A-n64-k9	1417	26.56	4.24	65.36	P-n20-k2	208	0.18	0.18	0.18
A-n65-k9	1184	3.69	1.01	12.21	P-n21-k2	208	0.19	0.19	0.19

A-n69-k9	1177	16.96	4.21	28.54	P-n22-k2	213	0.20	0.20	0.20
A-n80-k10	1803	33.70	6.34	116.94	P-n22-k8	601	0.19	0.12	0.29
B-n31-k5	694	0.23	0.19	0.47	P-n23-k8	527	0.29	0.17	0.47
B-n34-k5	789	0.29	0.27	0.33	P-n40-k5	468	0.47	0.44	0.72
B-n35-k5	986	0.23	0.22	0.26	P-n45-k5	512	2.17	0.51	5.97
B-n38-k6	823	0.32	0.27	0.49	P-n50-k7	563	0.92	0.50	1.48
B-n39-k5	561	0.34	0.30	0.52	P-n50-k8	614	1.32	0.42	2.82
B-n41-k6	838	2.96	0.30	6.36	P-n50-k10	695	3.06	0.98	8.78
B-n43-k6	779	1.69	0.43	2.88	P-n51-k10	736	1.96	0.44	6.52
B-n44-k7	943	0.93	0.46	2.47	P-n55-k7	583	1.98	0.60	3.42
B-n45-k5	739	0.61	0.53	0.74	P-n55-k8	624	2.92	0.80	9.46
B-n45-k6	668	0.38	0.37	0.40	P-n55-k10	718	14.52	1.13	49.25
B-n50-k7	758	1.48	0.44	3.28	P-n55-k15	945	1.91	0.99	3.56
B-n50-k8	1330	24.06	8.89	73.10	P-n60-k10	755	7.40	1.44	19.94
B-n51-k7	1027	2.26	0.54	5.66	P-n60-k15	1020	117.25	37.21	310.22
B-n52-k7	775	0.58	0.45	0.84	P-n65-k10	809	8.17	1.78	18.45
B-n56-k7	740	1.20	0.96	1.75	P-n70-k10	824	37.48	2.81	88.71
B-n57-k7	1132	2.02	0.76	4.79	P-n76-k4	590	7.49	2.33	20.40
B-n57-k9	1656	21.47	4.64	52.27	P-n76-k5	621	4.24	1.77	11.39
B-n63-k10	1588	19.13	2.17	56.77	P-n101-k4	681	6.84	4.50	15.75

EC.6.5. Raw BCP results for $\mathcal{D}^{card}$

Inst.	root LB	UB	time	Inst.	root LB	UB	time
A-n32-k5	857.0	857	3.79	B-n64-k9	852.0	<u>866</u>	7200.00
A-n33-k5	675.0	675	6.55	B-n66-k9	1319.0	1319	97.71
A-n33-k6	758.0	758	1.22	B-n67-k10	1086.0	1086	54.20

A-n34-k5	776.0	776	2.26	B-n68-k9	1298.0	1298	63.23
A-n36-k5	823.0	823	7.79	B-n78-k10	1261.0	1261	216.35
A-n37-k5	706.0	706	3.81	E-n13-k4	277.0	277	0.17
A-n37-k6	948.0	948	9.26	E-n22-k4	373.0	373	3.39
A-n38-k5	714.0	714	4.14	E-n23-k3	570.0	570	9.98
A-n39-k5	818.0	818	36.82	E-n30-k3	495.0	495	14.10
A-n39-k6	850.0	850	6.63	E-n31-k7	378.3	379	0.76
A-n44-k6	930.0	930	3.51	E-n33-k4	836.0	836	38.69
A-n45-k6	918.0	918	10.86	E-n51-k5	519.0	519	15.18
A-n45-k7	1163.0	1163	4.85	E-n76-k7	697.0	697	148.17
A-n46-k7	988.0	988	13.18	E-n76-k8	736.0	736	95.75
A-n48-k7	1129.0	1129	47.08	E-n76-k10	830.0	830	200.64
A-n53-k7	1019.0	1019	29.49	E-n76-k14	1020.0	1020	32.34
A-n54-k7	1169.0	1169	53.05	E-n101-k8	826.0	826	909.78
A-n55-k9	1107.0	1107	21.92	E-n101-k14	1107.0	1109	1977.15
A-n60-k9	1404.1	1408	176.50	F-n45-k4	736.0	736	85.10
A-n61-k9	1022.0	1022	34.40	F-n72-k4	236.0	236	583.44
A-n62-k8	1339.0	1339	106.29	M-n101-k10	918.0	918	25.98
A-n63-k9	1612.1	1618	334.82	M-n121-k7	1030.0	1030	450.81
A-n63-k10	1348.0	1348	56.41	P-n19-k2	195.0	195	0.28
A-n64-k9	1413.7	1414	35.36	P-n20-k2	208.0	208	0.52
A-n65-k9	1184.0	1184	91.31	P-n21-k2	208.0	208	0.71
A-n69-k9	1177.0	1177	35.08	P-n22-k2	213.0	213	1.35
A-n80-k10	1795.0	1795	248.47	P-n22-k8	601.0	601	0.75
B-n31-k5	694.0	694	1.36	P-n23-k8	527.0	527	0.24

B-n34-k5	789.0	789	6.44	P-n40-k5	468.0	468	9.59
B-n35-k5	986.0	986	5.37	P-n45-k5	512.0	512	16.64
B-n38-k6	823.0	823	15.59	P-n50-k7	563.0	563	8.01
B-n39-k5	561.0	561	26.39	P-n50-k8	614.0	614	45.16
B-n41-k6	838.0	838	1876.79	P-n50-k10	695.0	695	5.49
B-n43-k6	779.0	779	25.14	P-n51-k10	736.0	736	8.61
B-n44-k7	943.0	943	25.11	P-n55-k7	583.0	583	22.13
B-n45-k5	739.0	739	46.24	P-n55-k8	624.0	624	14.93
B-n45-k6	668.0	668	19.24	P-n55-k10	718.0	718	11.86
B-n50-k7	758.0	758	6.31	P-n55-k15	945.0	945	4.70
B-n50-k8	1330.0	1330	19.70	P-n60-k10	755.0	755	29.65
B-n51-k7	1010.1	1027	7200.00	P-n60-k15	1020.0	1020	20.87
B-n52-k7	775.0	775	22.00	P-n65-k10	809.0	809	66.89
B-n56-k7	740.0	740	23.78	P-n70-k10	824.0	824	63.11
B-n57-k7	1112.8	1133	7200.00	P-n76-k4	590.0	590	267.42
B-n57-k9	1656.0	1656	77.70	P-n76-k5	621.0	621	284.10
B-n63-k10	1578.9	1587	843.21	P-n101-k4	681.0	681	2096.77

* Root LB value correspond to gap 1 value on Table 4.

** Only underlined UB values are not proved to be optimal